Numerical detailing of the mechanism responsible for artificial heating of the ionosphere by powerful high frequency radio waves

Abstract

The effect of a standing high-power high-frequency radio wave on the behavior of the F-layer ionospheric plasma is numerically investigated with the help of the mathematical model, developed earlier in the Polar Geophysical Institute. The mathematical model is based on a numerical solution of the Vlasov-Poisson system of equations by using the macroparticle method. The results of model simulations indicate that a presence of a standing high-power high-frequency radio wave ought to influence significantly on the behavior of the bulk flow velocities of electrons and positive ions, with considerable differences between mentioned velocities taking place at the levels of the wave's loops, whereas, mentioned velocities being equal and negligible at the levels of the nodal points. As a consequence of the different behavior of the bulk flow velocities of electrons and positive ions, intensive heating of the F-layer ionospheric plasma ought to arise at the levels of the loops of a wave. On the contrary, at the levels of the nodal points, the ionospheric plasma ought to stay undisturbed.

Keywords

Ionospheric Plasma, Active Experiments, Modeling and Forecasting

1. Introduction

Artificial heating experiments by powerful high frequency (HF) radio waves, pumped into the ionosphere by ground-based ionospheric heaters, were successfully used during the last four decades for the investigations of the ionospheric plasma's properties. For fulfillment of these investigations, some ground-based ionospheric heaters have been built not only in the mid-latitudes (Platteville, Arecibo, Nizhny Novgorod, etc.) but also in the high-latitudes, namely, near Monchegorsk, Kola Peninsula, near Tromso, Scandinavia, near Fairbanks, Alaska, near Gakona, Alaska, and near Longyearbyen, Svalbard. The obtained experimental data indicated that powerful HF radio waves, pumped into the ionosphere, can produce significant large-scale variations in the electron temperatures and densities at F-layer altitudes [1-22].

To study the influence of high-power HF radio waves on the behavior of the ionospheric plasma, mathematical models may be applied. Model simulations of the large-scale F-layer modification by powerful HF radio waves have been performed in some studies (in particular, see [23-28]). Also, in the Polar Geophysical Institute (PGI), a mathematical model of the F-region ionosphere, which can be affected by a powerful HF wave, has been developed [29]. This model has been utilized to study the influence of various parameters of high-power HF radio waves on the large-scale modification of the F-region ionosphere [29-36].

In the near-Earth plasma, magnetic field aligned super-small-scale irregularities in the concentration of charged particles are often observed. These irregularities either are naturally present or may be artificially produced as a result of active experiments in the near-Earth plasma. The parameters of the magnetic field aligned super-small-scale irregularities in the concentration of charged particles have been described in details by Wong et al. [37]. These authors have pointed out that diametrical sizes of these irregularities are several Debye lengths (no more that about 100), while the disturbances of the density of charged particles in them can reach some tens of percentages.

To investigate the behavior of these super-small-scale irregularities, computational studies may be applied. In particular, the formation of the super-small-scale irregularities was considered and simulated in the study by Eliasson and Stenflo [38]. Besides, in the PGI, a mathematical model, based on a numerical solution of the Vlasov-Poisson system of equations by using the macroparticle method, has been developed [39]. The time evolution of the super-small-scale irregularities in the electron concentration, created initially in the F-region ionospheric plasma, has been studied under various geophysical conditions with the help of this mathematical model [39-42]. In the study by Mingalev et al. [43], this mathematical model has been utilized for studying the time evolution of the super-small-scale irregularity in the electron concentration under action of a high-power HF radio wave, pumped into the ionosphere by a ground-based ionospheric heater. The simulation results indicated that a high-power HF radio wave influences not only on the evolution of the irregularity but also on the behavior of the ambient ionospheric plasma.

In the present study, the mathematical model, intended for studying the time evolution of the super-small-scale irregularities in the F-layer ionospheric plasma, is utilized for numerical investigation of the effect of high-power HF radio waves on the behavior of the ambient ionospheric plasma. The present work is the continuation of the

investigation begun in the study of Mingalev et al. [43], with new simulation results, concerning the mechanism responsible for artificial heating of ionospheric plasma by powerful HF radio waves, being submitted in the present paper.

2. Mathematical Model

The ionospheric plasma at F-layer altitudes is assumed to be a rarefied compound consisting of electrons and positive ions in the presence of a strong, external, uniform magnetic field. Utilized mathematical model, intended for studying the time evolution of the super-small-scale irregularities in the F-layer ionospheric plasma, takes into account that the mean free path of particles (electrons and ions) between successive collisions is much more than the cross-section diameters of these irregularities. Therefore, the plasma is supposed to be collisionless. Kinetic processes in such plasma are described by the Vlasov-Poisson system of equations, with the Vlasov equations describing the distribution functions of charged particles and the Poisson equation governing the self-consistent electric field. Detailed description of these equations may be found, for example, in the studies by Hockney and Eastwood [44], and Birdsall and Langdon [45]. The system of equations may be written as follows:

$$\frac{\partial f_a}{\partial t}+\left(\mathbf{v},\frac{\partial f_a}{\partial \mathbf{x}}\right)+\frac{q_a}{m_a}\left(\mathbf{E}+\left[\mathbf{v}\times\mathbf{B}_0\right],\frac{\partial f_a}{\partial \mathbf{v}}\right)=0, \qquad a=i,e \qquad (1)$$

$$\Delta\varphi(\mathbf{x},t)=-\frac{1}{\varepsilon_0}\rho(\mathbf{x},t), \qquad (2)$$

$$\mathbf{E}(\mathbf{x},t)=-\nabla\varphi(\mathbf{x},t), \qquad \rho(\mathbf{x},t)=e_0(n_i-n_e), \qquad n_a(\mathbf{x},t)=\int f_a(t,\mathbf{x},\mathbf{v})\ d\mathbf{v},$$

where $f_a(t,\mathbf{x},\mathbf{v})$, $n_a(\mathbf{x},t)$, m_a, and q_a are, respectively, the distribution function, concentration, mass, and charge of particles of type a, $\mathbf{x}$ is the space coordinate vector, $\mathbf{v}$ is the velocity, $\mathbf{B}_0$ is the external magnetic field, $\mathbf{E}$ is the self-consistent electric field, $\varphi(\mathbf{x},t)$ is the electric field potential, $\rho(\mathbf{x},t)$ is the electric charge density, ε_0 is the dielectric constant of free space, and e_0 is the proton charge. The Vlasov equation, (1), describes the behavior of the distribution function of electrons ($a = e$) and ions ($a = i$), whereas Poisson equation, (2), describes the self consistent electric field in the plasma. For numerical solving of the Vlasov equations, (1), a macroparticle method is used. For numerical solving of the Poisson equation, (2), a finite-difference method is utilized.

As a consequence of specific configuration of magnetic field aligned super-small-scale irregularities in the concentration of charged particles, it is sufficient to consider a two dimensional flow of plasma in a plane perpendicular to a magnetic field line. Therefore, the utilized mathematical model is two-dimensional. In the time-dependent model calculations, a two-dimensional simulation region, lain in the plane perpendicular to the magnetic field line, is a square and its side length is equal to 128 Debye lengths of the plasma. The quantity of the grid cells is 1024×1024 and the average number of macro-particles in the Debye cell for the model plasma is 2^{15}. More complete details of the utilized mathematical model may be found in the studies of Mingalev et al. [39-43].

3. Presentation and Discussion of Results

The utilized mathematical model can describe the behavior of the ionospheric plasma under various conditions. The results of modeling to be presented in this work were obtained using the input parameters of the model typical for the nocturnal F-region ionospheric plasma at the level of 300 km. In particular, the value of the non-disturbed electron concentration (equal to the positive ion concentration), n_0, is equal to 10^{11} m^{-3}. The electron and ion temperatures are assumed to be equal to 1213 K and 930 K, respectively. At the initial moment, the bulk flow velocities of electrons and positive ions, $\boldsymbol{U_e}$ and $\boldsymbol{U_i}$ respectively, are supposed to be zero. The value of the magnetic field is $4.4\cdot10^{-5}$ T. Under chosen parameters of the ionospheric plasma, the equilibrium plasma frequency, ω^0_{pe}, is $1.78\cdot10^7$ s^{-1}, the frequency of cyclotron oscillations of electrons, ω_{ce}, is $7.74\cdot10^6$ s^{-1}, the Debye length of the plasma, λ^0_{De}, is equal to $7.6\cdot10^{-3}$ m, the equilibrium period of Langmuir oscillations of electrons, T_{pe}, is $3.52\cdot10^{-7}$ s, the period of cyclotron oscillations of electrons, T_{ce}, is approximately a factor of 2.3 larger than the equilibrium period of Langmuir oscillations of electrons ($T_{ce} \approx 2.3\cdot T_{pe}$), and the mean free time of electron between successive collisions with other particles is larger than the equilibrium period of Langmuir oscillations of electrons by a factor of about 1047. It may be noted that the pointed out parameters of the ionospheric plasma have been used in the study by Mingalev et al. [43], also.

The simulation results to be presented in this paper were obtained for two distinct on principle situations. The external electric field is absent for the first situation. Unlike, the external electric field, which represents a high-power HF radio wave, pumped into the ionosphere by a ground-based ionospheric heater, is present for the second situation. It is assumed that this high-power HF radio wave illuminates the two-dimensional simulation region.

It is assumed that the HF radio wave, radiated by a ground-based ionospheric heater, propagates upwards along a magnetic field line up to the reflection point, turns back, and propagates towards the Earth's surface along a magnetic field line. It is supposed that the upward and downward HF radio waves form a standing wave. A schematic representation of a standing high-power HF radio wave, utilized for an artificial heating experiment and excited by a ground-based ionospheric heater, is presented in Figure 1. It can be noticed that the formation of a standing wave is more probable at high latitudes where the direction of magnetic field is close to vertical.

The simulation region of the utilized mathematical model is two-dimensional and it lies in the plane perpendicular to the magnetic field line. It is supposed that the vector of the HF wave's electric field, **E**, lies in the plane of the simulation region, with the projection of **E,** perpendicular to the simulation region, being absent. The disturbing HF radio wave is assumed to be ordinary and to have the frequency of the electron hybrid resonance, namely, $\omega_0 = [(\omega^0_{pe})^2 + (\omega_{ce})^2]^{1/2}$. Therefore, the frequency of the disturbing HF radio wave, ω_0, is approximately a factor of 1.09 larger than the equilibrium plasma frequency ($\omega_0 \approx 1.09 \cdot \omega^0_{pe}$), with the wave length being close to 100 m. It is assumed that the module of the vector of the HF wave's electric field, after the initial moment, increases smoothly and reaches the maximal value of 0.49 V/m during the time interval of five periods of Langmuir oscillations of electrons.

Let us consider the first situation, when a standing high-power HF radio wave, excited by a ground-based ionospheric heater, is absent. The results of simulation indicated that, for this situation, the distribution functions of charged particles as well as self-consistent electric field in the ionospheric plasma were retained invariable. As a consequence, the bulk flow velocities of electrons and positive ions, $\boldsymbol{U_e}$ and $\boldsymbol{U_i}$, were retained close to zero at all levels of the F region.

Let us consider the second situation, when the plane standing high-power HF radio wave, excited by a ground-based ionospheric heater, is present. The time variations of two perpendicular components of the vector of the HF wave's electric field at one point of the simulation region, when this region is situated at the level of a loop of the wave, are shown in Figure 2. At other points of the simulation region, the behavior of the vector of the HF wave's electric field is analogous. In each point of the two-dimensional simulation region, the vector of the HF wave's electric field, **E**, rotates with the frequency equal to ω_0, with this fact being seen from Figure 2 as a consequence of time displacement of the maximal values of perpendicular components of the vector of the HF wave's electric field. It should be emphasized that chosen maximal value of the module of the vector of the HF wave's electric field is quite attainable, for example, for the heating facility near Tromso, Scandinavia. Also, it is seen from Figure 2 that, for the first situation, the electric field components are absent at the considered point of the simulation region.

The time variations of perpendicular components of the vectors of the bulk flow velocities of the positive ions and electrons at some points of the simulation region, when this region is situated at the level of a loop of the wave, are shown in Figures 3 and 4, respectively. From these Figures, it can be seen that, at the level of a loop of the wave, the vectors of the bulk flow velocities of the positive ions and electrons rotate with the frequency equal to the frequency of the disturbing HF radio wave, ω_0. These facts follow from time displacements of the maximal values of the perpendicular components of the vectors of the bulk flow velocities of the positive ions and electrons.

The rotation of the vectors of the bulk flow velocities of the positive ions and electrons is not unexpected. The ionospheric plasma at F-layer altitudes is known to be strongly magnetized. Therefore, the bulk flow velocities of the positive ions and electrons are strongly affected by the electric field **E**, with the plasma transport perpendicular to the magnetic field lines following **E×B** direction. As a consequence of the rotation of the vector of the HF wave's electric field **E**, the vectors of the bulk flow velocities of the positive ions and electrons rotate, too, at levels of loops of the disturbing HF radio wave.

The simulation results indicated that the rotation of the vectors of the bulk flow velocities of the positive ions and electrons take place not only at some points of the simulation region, used in Figures 3 and 4, but also at each point of the two-dimensional simulation region. This fact can be confirmed by Figure 5, where the spatial distributions of the vector of the bulk flow velocity of electrons are shown for some successive moments in all simulation region, when this region is situated at the level of a loop of the radio wave. It should be emphasized that, at the levels of the nodal points, the vectors of the bulk flow velocities of the positive ions and electrons are retained close to zero.

It is known that, as a consequence of strong magnetization of the positive ions and electrons in the ionospheric plasma at F-layer altitudes, the bulk flow velocities of the positive ions and electrons in the **E×B** direction ought to be equal, when the electric field **E** varies in the course of time slowly. The obtained simulation results indicated that absolute values of vectors of flow velocities of electrons are much more than modules of vectors of flow velocities of positive ions (Figures 3 and 4), when the electric field **E** varies in the course of time very rapidly. The modules of vectors of flow velocities of electrons can reach values of some km/s. As a consequence of great differences

between the bulk flow velocities of electrons and positive ions, intensive Joule heating of the F-layer ionospheric plasma ought to arise at the levels of the loops of a wave.

In the F-layer ionosphere, the neutral particles are known to be present whose velocities are much less than bulk flow velocities of electrons, obtained in the described simulations. Due to high differences between the bulk flow velocities of electrons and neutral particles, the frictional heating of the ionospheric plasma ought to arise at the levels of the loops of a wave, with this frictional heating being a result of elastic collisions between particles.

It can be noticed that perceptible Joule heating and frictional heating of the ionospheric plasma ought to be absent at the levels of the nodal points of a standing high-power HF radio wave.

The intense high-power radio waves, utilized for artificial heating experiments and pumped into the ionosphere by ground-based ionospheric heaters, are decameter waves. Therefore, in a standing radio wave, formed below the reflection point, the distance between neighbouring loops, which is equal to half of a wave length, ought to be less than approximately 50 m. Analogous distances take place between neighbouring nodes of a wave (Figure 1). Consequently, it may be expected that the layers of heated ionospheric plasma are present in the F region below the reflection point. Between these hot layers, the layers of undisturbed ionospheric plasma ought to be present. Thicknesses of these hot and undisturbed layers ought to be less than the half of a wave length.

4. Conclusions

The influence of a high-power HF radio waves, pumped into the ionosphere by ground-based ionospheric heaters during the periods of active experiments, on the behavior of the F-layer ionospheric plasma has been studied with the help of the mathematical model, developed earlier in the PGI. The utilized mathematical model is based on the numerical solution of the Vlasov-Poisson system of equations, with the Vlasov equations describing the distribution functions of charged particles and the Poisson equation governing the self-consistent electric field. The applied mathematical model allows us to investigate numerically kinetic processes in ionospheric plasma. The simulation results have indicated that a presence of a standing high-power HF radio wave ought to influence significantly on the behavior of the bulk flow velocities of electrons and positive ions. At the levels of the loops of the wave, the vectors of the bulk flow velocities of the positive ions and electrons rotate with the frequency equal to the frequency of the disturbing HF radio wave. It turned out that considerable differences between modules of bulk flow velocities of electrons and positive ions take place at the levels of the wave's loops, whereas, mentioned velocities are equal and negligible at the levels of the nodal points. As a consequence, intensive heating of the F-layer ionospheric plasma ought to arise at the levels of the loops of a wave. On the contrary, at the levels of the nodal points, the ionospheric plasma ought to stay undisturbed. Thus, in the present paper, new details of the mechanism responsible for artificial heating of ionospheric plasma by powerful HF radio waves, pumped into the ionosphere by ground-based ionospheric heaters, have been submitted.

References

[1] Utlaut, W.F. and Violette, E.J. (1974) A Summary of Vertical Incidence Radio Observations of Ionospheric Modification. *Radio Science*, **9**, 895-903. http://dx.doi.org/10.1029/RS009i011p00895

[2] Gordon, W.E. and Carlson, H.C. (1974) Arecibo Heating Experiments. *Radio Science*, **9**, 1041-1047. http://dx.doi.org/10.1029/RS009i011p01041

[3] Kapustin, I.N., Pertsovskii, R.A., Vasil'ev, A.N., Smirnov, V.S., Raspopov, O.M., Solov'eva, L.E., Ul'yanchenko, A.A., Arykov, A.A. and Galachova, N.V. (1977) Generation of Radiation at Combination Frequencies in the Region of the Auroral Electric Jet. *JETP Letters*, **25**, 228-231.

[4] Mantas, G.P., Carlson, H.C. and La Hoz, C.H. (1981) Thermal Response of F-Region Ionosphere in Artificial Modification Experiments by HF Radio Waves. *Journal of Geophysical Research*, **86**, 561-574. http://dx.doi.org/10.1029/JA086iA02p00561

[5] Stubbe, P. and Kopka, H. (1983) Summary of Results Obtained with the Tromso Heating Facility. *Radio Science*, **18**, 831-834. http://dx.doi.org/10.1029/RS018i006p00831

[6] Jones, T.B., Robinson, T.R., Stubbe, P. and Kopka, H. (1986) EISCAT Observations of the Heated Ionosphere. *Journal of Atmospheric and Terrestrial Physics*, **48**, 1027-1035. http://dx.doi.org/10.1016/0021-9169(86)90074-7

[7] Djuth, F.T., Thide, B., Ierkic, H.M. and Sulzer, M.P. (1987) Large F-Region Electron-Temperature Enhancements Generated by High-Power HF Radio Waves. *Geophysical Research Letters*, **14**, 953-956. http://dx.doi.org/10.1029/GL014i009p00953

[8] Duncan, L.M., Sheerin, J.P. and Behnke, R.A. (1988) Observations of Ionospheric Cavities Generated by High-Power Radio Waves. *Physical Review Letters*, **61**, 239-242. http://dx.doi.org/10.1103/PhysRevLett.61.239

[9] Hansen, J.D., Morales, G.J., Duncan, L.M. and Dimonte, G. (1992) Large-Scale HF-Induced Ionospheric Modification: Experiments. *Journal of Geophysical Research*, **97**, 113-122. http://dx.doi.org/10.1029/91JA02403

[10] Mantas, G.P. (1994) Large 6300-Å Airglow Intensity Enhancements Observed in Ionosphere Heating Experiments Are Exited by Thermal Electrons. *Journal of Geophysical Research*, **99**, 8993-9002. http://dx.doi.org/10.1029/94JA00347

[11] Honary, F., Stocker, A.J., Robinson, T.R., Jones, T.B. and Stubbe, P. (1995) Ionospheric Plasma Response to HF Radio Waves Operating at Frequencies Close to the Third Harmonic of the Electron Gyrofrequency. *Journal of Geophysical Research*, **100**, 21489-21501. http://dx.doi.org/10.1029/95JA02098

[12] Robinson, T.R., Honary, F., Stocker, A.J., Jones, T.B. and Stubbe, P. (1996) First EISCAT Observations of the Modification of F-Region Electron Temperatures during RF Heating at Harmonics of the Electron Gyro Frequency. *Journal of Atmospheric and Terrestrial Physics*, **58**, 385-395. http://dx.doi.org/10.1016/0021-9169(95)00043-7

[13] Stubbe, P. (1996) Review of Ionospheric Modification Experiments at Tromso. *Journal of Atmospheric and Terrestrial Physics*, **58**, 349-368. http://dx.doi.org/10.1016/0021-9169(95)00041-0

[14] Belikovich, V.V., Benediktov, E.A., Tolmacheva, A.V. and Bakhmet'eva, N.V. (1999) Studying the Ionosphere Using Artificial Periodic Irregularities. IAP RAS, Nizhni Novgorod. (In Russian)

[15] Gustavsson, B., Sergienko, T., Rietveld, M.T., Honary, F., Steen, A., Brandstrom, B.U.E., Leyser, T.B., Aruliah, A.L., Aso, T., Ejiri, M. and Marple, S. (2001) First Tomographic Estimate of Volume Distribution of HF-Pump Enhanced Airglow Emission. *Journal of Geophysical Research*, **106**, 29105-29124. http://dx.doi.org/10.1029/2000JA900167

[16] Rietveld, M.T., Kosch, M.J., Blagoveshchenskaya, N.F., Kornienko, V.A., Leyser, T.B. and Yeoman, T.K. (2003) Ionospheric Electron Heating, Optical Emissions, and Striations Induced by Powerful HF Radio Waves at High Latitudes: Aspect Angle Dependence. *Journal of Geophysical Research*, **108**, 1141. http://dx.doi.org/10.1029/2002JA009543

[17] Ashrafi, M., Kosch, M.J., Kaila, K. and Isham, B. (2007) Spatiotemporal Evolution of Radio Wave Pump-Induced Ionospheric Phenomena Near the Fourth Electron Gyroharmonic. *Journal of Geophysical Research*, **112**, A05314. http://dx.doi.org/10.1029/2006JA011938

[18] Dhillon, R.S., Robinson, T.R. and Yeoman, T.K. (2007) EISCAT Svalbard Radar Observations of SPEAR-Induced Eand F-Region Spectral Enhancements in the Polar Cap Ionosphere. *Annales Geophysicae*, **25**, 1801-1814. http://dx.doi.org/10.5194/angeo-25-1801-2007

[19] Kosch, M.J., Pedersen, T., Rietveld, M.T., Gustavsson, B., Grach, S.M. and Hagfors, T. (2007) Artificial Optical Emissions in the High-Latitude Thermosphere Induced by Powerful Radio Waves: An Observational Review. *Advances in Space Research*, **40**, 365-376. http://dx.doi.org/10.1016/j.asr.2007.02.061

[20] Yeoman, T.K., Blagoveshchenskaya, N., Kornienko, V., Robinson, T.R., Dhillon, R.S., Wright, D.M. and Baddeley, L.J. (2007) SPEAR: Early Results from a Very High Latitude Ionospheric Heating Facility. *Advances in Space Research*, **40**, 384-389. http://dx.doi.org/10.1016/j.asr.2007.02.059

[21] Clausen, L.B.N., Yeoman, T.K., Wright, D.M., Robinson, T.R., Dhillon, R.S. and Gane, S.C. (2008) First Results of a ULF Wave Injected on Open Field Lines by Space Plasma Exploration by Active Radar (SPEAR). *Journal of Geophysical Research*, **113**, A01305. http://dx.doi.org/10.1029/2007JA012617

[22] Pedersen, T., Esposito, R., Kendall, E., Sentman, D., Kosch, M., Mishin, E. and Marshall, R. (2008) Observations of Artificial and Natural Optical Emissions at the HAARP Facility. *Annales Geophysicae*, **26**, 1089-1099. http://dx.doi.org/10.5194/angeo-26-1089-2008

[23] Meltz, G. and LeLevier, R.E. (1970) Heating the F-Region by Deviative Absorption of Radio Waves. *Journal of Geophysical Research*, **75**, 6406-6416. http://dx.doi.org/10.1029/JA075i031p06406

[24] Perkins, F.W. and Roble, R.G. (1978) Ionospheric Heating by Radio Waves: Predictions for Arecibo and the Satellite Power Station. *Journal of Geophysical Research*, **83**, 1611-1624. http://dx.doi.org/10.1029/JA083iA04p01611

[25] Mantas, G.P., Carlson, H.C. and La Hoz, C.H. (1981) Thermal Response of F-Region Ionosphere in Artificial Modification Experiments by HF Radio Waves. *Journal of Geophysical Research*, **86**, 561-574. http://dx.doi.org/10.1029/JA086iA02p00561

[26] Bernhardt, P.A. and Duncan, L.M. (1982) The Feedback-Diffraction Theory of Ionospheric Heating. *Journal of Atmospheric and Terrestrial Physics*, **44**, 1061-1074. http://dx.doi.org/10.1016/0021-9169(82)90018-6

[27] Hansen, J.D., Morales, G.J. and Maggs, J.E. (1989) Daytime Saturation of Thermal Cavitons. *Journal of Geophysical Research*, **94**, 6833-6840. http://dx.doi.org/10.1029/JA094iA06p06833

[28] Vas'kov, V.V., Dimant, Ya.S. and Ryabova, N.A. (1993) Magnetospheric Plasma Thermal Perturbations Induced by Resonant Heating of the Ionospheric F-Region by High-Power Radio Wave. *Advances in Space Research*, **13**, 25-33. http://dx.doi.org/10.1016/0273-1177(93)90047-F

[29] Mingaleva, G.I. and Mingalev, V.S. (1997) Response of the Convecting High-Latitude F Layer to a Powerful HF Wave. *Annales Geophysicae*, **15**, 1291-1300. http://dx.doi.org/10.1007/s00585-997-1291-8

[30] Mingaleva, G.I. and Mingalev, V.S. (2002) Modeling the Modification of the Nighttime High-Latitude F-Region by Powerful HF Radio Waves. *Cosmic Research*, **40**, 55-61. http://dx.doi.org/10.1023/A:1014299902287

[31] Mingaleva, G.I. and Mingalev, V.S. (2003) Simulation of the Modification of the Nocturnal High-Latitude F Layer by Powerful HF Radio Waves. *Geomagnetism and Aeronomy*, **43**, 816-825. (Russian Issue)
[32] Mingaleva, G.I., Mingalev, V.S. and Mingalev, I.V. (2003) Simulation Study of the High-Latitude F-Layer Modification by Powerful HF Waves with Different Frequencies for Autumn Conditions. *Annales Geophysicae*, **21**, 1827-1838. http://dx.doi.org/10.5194/angeo-21-1827-2003
[33] Mingaleva, G.I., Mingalev, V.S. and Mingalev, I.V. (2009) Model Simulation of the Large-Scale High-Latitude F-Layer Modification by Powerful HF Waves with Different Modulation. *Journal of Atmospheric and Solar-Terrestrial Physics*, **71**, 559-568. http://dx.doi.org/10.1016/j.jastp.2008.11.007
[34] Mingaleva, G.I., Mingalev, V.S. and Mingalev, O.V. (2012) Simulation Study of the Large-Scale Modification of the Mid-Latitude F-Layer by HF Radio Waves with Different Powers. *Annales Geophysicae*, **30**, 1213-1222. http://dx.doi.org/10.5194/angeo-30-1213-2012
[35] Mingaleva, G.I. and Mingalev, V.S. (2013) Simulation Study of the Modification of the High-Latitude Ionosphere by Powerful High-Frequency Radio Waves. *Journal of Computations and Modelling*, **3**, 287-309.
[36] Mingaleva, G.I. and Mingalev, V.S. (2014) Model Simulation of Artificial Heating of the Daytime High-Latitude F-Region Ionosphere by Powerful High-Frequency Radio Waves. *International Journal of Geosciences*, Volume 2014(5), 363-374.
[37] Wong, A.Y., Santoru, J., Darrow, C., Wang, L. and Roederer, J.G. (1983) Ionospheric Cavitons and Related Nonlinear Phenomena. *Radio Science*, **18**, 815-830. http://dx.doi.org/10.1029/RS018i006p00815
[38] Eliasson, B. and Stenflo, L. (2008) Full-Scale Simulation Study of the Initial Stage of Ionospheric Turbulence. *Journal of Geophysical Research*, **113**, Article ID: A02305. http://dx.doi.org/10.1029/2007JA012837
[39] Mingalev, O.V., Mingalev, I.V. and Mingalev, V.S. (2006) Two-Dimensional Numerical Simulation of Dynamics of Small-Scale Irregularities in the Near-Earth Plasma. *Cosmic Research*, **44**, 398-408. http://dx.doi.org/10.1134/S0010952506050030
[40] Mingalev, O.V., Mingaleva, G.I., Melnik, M.N. and Mingalev, V.S. (2010) Numerical Modeling of the Behavior of Super-Small-Scale Irregularities in the Ionospheric F2 Layer. *Geomagnetism and Aeronomy*, **50**, 643-654. http://dx.doi.org/10.1134/S0016793210050117
[41] Mingalev, O.V., Mingaleva, G.I., Melnik, M.N. and Mingalev, V.S. (2011) Numerical Simulation of the Time Evolution of Small-Scale Irregularities in the F-Layer Ionospheric Plasma. *International Journal of Geophysics*, **2011**, Article ID: 353640. http://dx.doi.org/10.1155/2011/353640
[42] Mingalev, O.V., Melnik, M.N. and Mingalev, V.S. (2015) Numerical Modeling of the Time Evolution of Super-Small-Scale Irregularities in the Near-Earth Rarefied Plasma. *International Journal of Geosciences*, **6,** 67-78.
[43] Mingalev, O.V., Melnik, M.N. and Mingalev, V.S. (2016) A Simulation Study of the Effect of Powerful High-Frequency Radio Waves on the Behavior of Super-Small-Scale Irregularities in the F-Layer Ionospheric Plasma, *World Journal of Research and Review*, **3**(5), 01-09.
[44] Hockney, R.W. and Eastwood, J.W. (1981) Computer Simulation Using Particles. McGraw-Hill, New York.
[45] Birdsall, C.K. and Langdon, A.B. (1985) Plasma Physics via Computer Simulation. McGraw-Hill, New York.

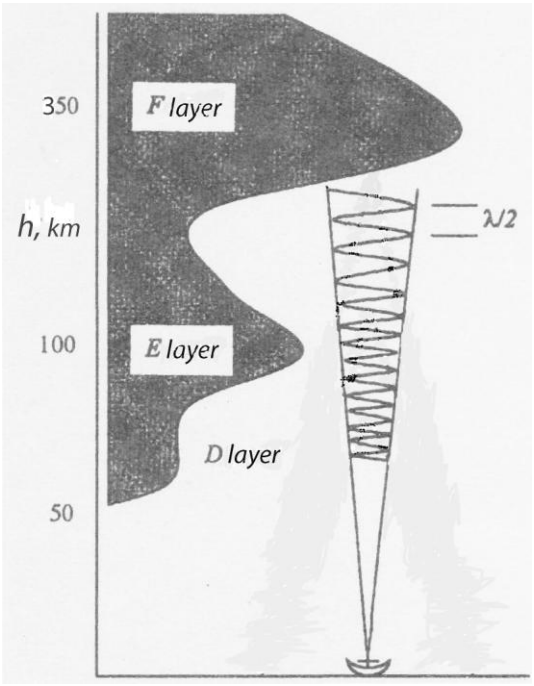

Fig 1. An exaggerated representation of a standing high-power HF radio wave, utilized for an artificial heating experiment and excited by a ground-based ionospheric heater [14]. A length of a wave, emitted by an ionospheric heater, is denoted by λ.

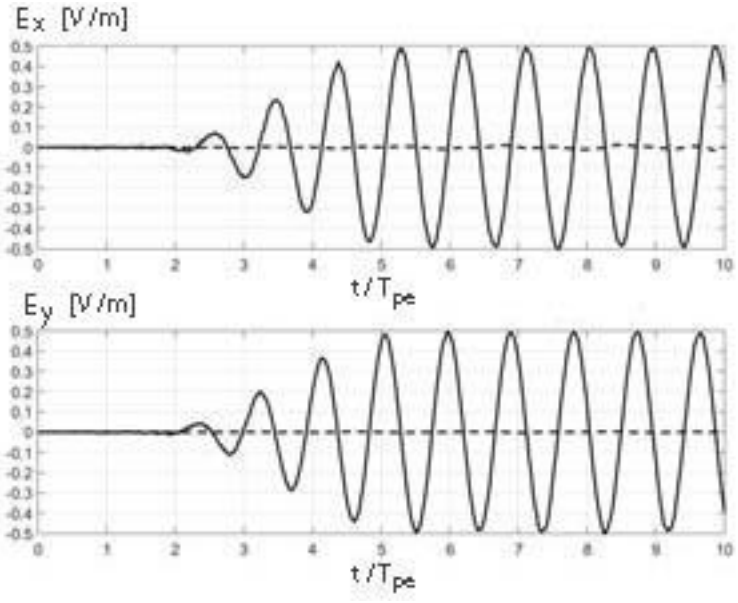

Fig. 2. The time variations of two perpendicular components of the vector of the HF wave's electric field, namely E_x (top panel) and E_y (bottom panel), lain in the simulation region, when this region is situated at the level of a loop of the wave, and calculated at the point, displaced from the center of the simulation region in the $\boldsymbol{X}$ direction for a distance of sixteen Debye lengths $\left(16 \cdot \lambda_{De}^{0}\right)$. For the first situation, correspondent to absence of an external electric field, the results are shown by dashed lines, whereas, for the second situation, correspondent to presence of the standing high-power HF radio wave, the results are shown by solid lines. The electric field components are given in V/m. The normalized time, t/T_{pe}, that is, the time in units of the equilibrium period of Langmuir oscillations of electrons, T_{pe}, is shown on the abscissas.

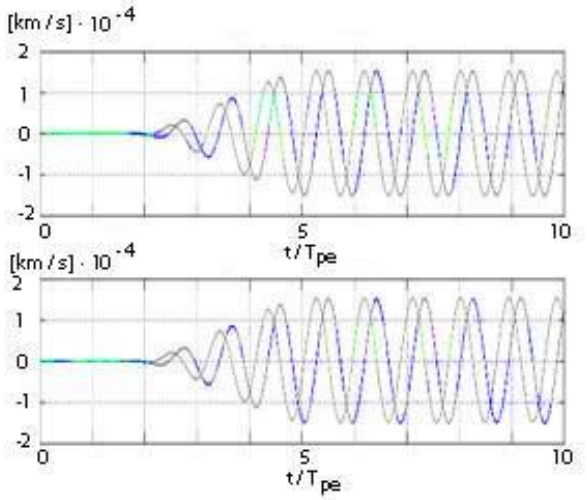

Fig. 3. The time variations of two perpendicular components of the vector of the bulk flow velocity of the positive ions, namely U_{ix} (blue lines) and U_{iy} (green lines), lain in the simulation region, when this region is situated at the level of a loop of the radio wave, and calculated for the second situation, correspondent to presence of the standing high-power HF radio wave. The results, calculated at the point, displaced from the center of the simulation region in the ***X*** direction for a distance of thirty Debye lengths $\left(30\cdot\lambda_{De}^{0}\right)$, are shown at the top panel. The results, calculated at the point, displaced from the center of the simulation region in the ***Y*** direction for a distance of thirty Debye lengths $\left(30\cdot\lambda_{De}^{0}\right)$, are shown at the bottom panel. The components of the vector of the bulk flow velocity of the positive ions are given in [km/s]·10^{-4}. The normalized time, t/T_{pe}, that is, the time in units of the equilibrium period of Langmuir oscillations of electrons, T_{pe}, is shown on the abscissas.

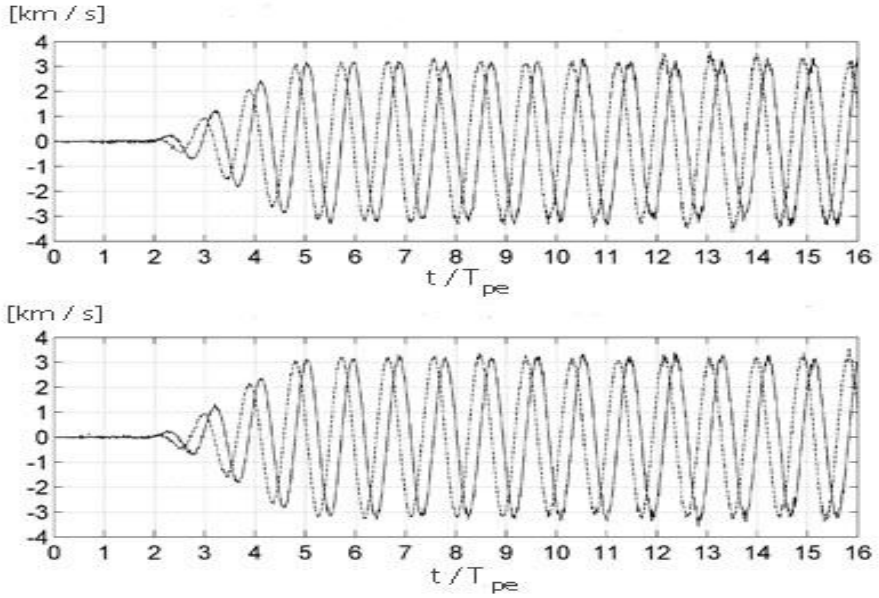

Fig. 4. The time variations of two perpendicular components of the vector of the bulk flow velocity of electrons, namely U_{ex} (solid lines) and U_{ey} (dashed lines), lain in the simulation region, when this region is situated at the level of a loop of the radio wave, and calculated for the second situation, correspondent to presence of the standing high-power HF radio wave. The results, calculated at the point, displaced from the center of the simulation region in the ***X*** direction for a distance of thirty Debye lengths $\left(30 \cdot \lambda_{De}^{0}\right)$, are shown at the top panel. The results, calculated at the point, displaced from the center of the simulation region in the ***Y*** direction for a distance of thirty Debye lengths $\left(30 \cdot \lambda_{De}^{0}\right)$, are shown at the bottom panel. The components of the vector of the bulk flow velocity of electrons are given in km/s. The normalized time, t / T_{pe}, that is, the time in units of the equilibrium period of Langmuir oscillations of electrons, T_{pe}, is shown on the abscissas.

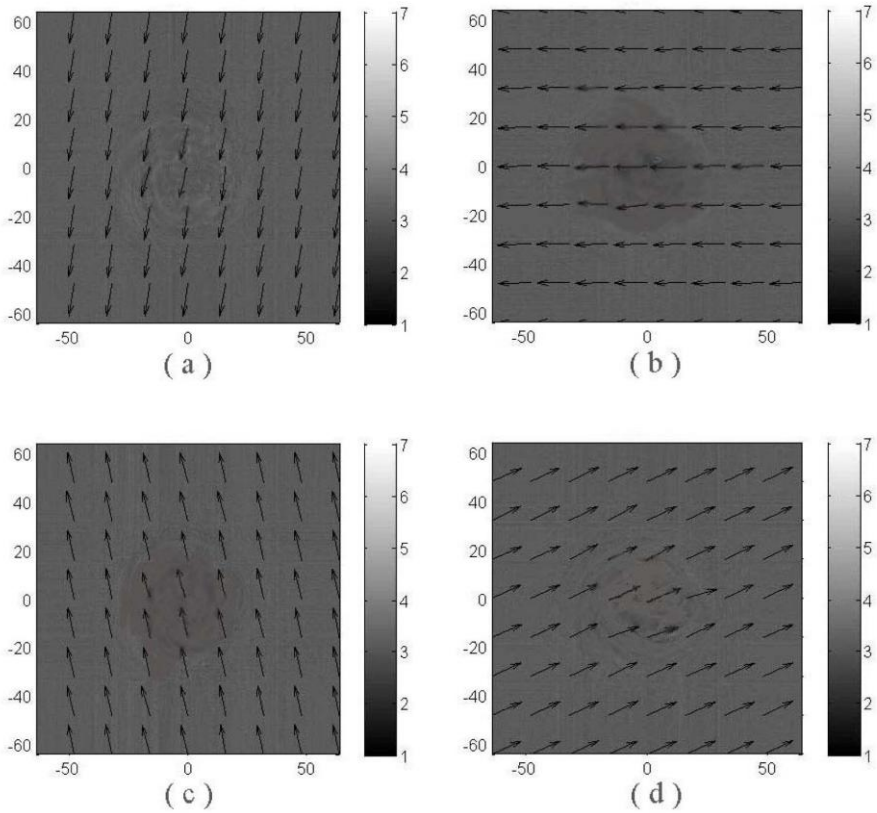

Fig.5. The spatial distributions of the vector of the bulk flow velocity of electrons, $\boldsymbol{U_e}$, lain in the simulation region, when this region is situated at the level of a loop of the radio wave, and calculated for the second situation, correspondent to presence of the standing high-power HF radio wave. The normalized distances, $\boldsymbol{X}/\lambda_{De}^{0}$ and $\boldsymbol{Y}/\lambda_{De}^{0}$, that is, the distances in units of the Debye length, λ_{De}^{0}, from the central point of the simulation region are shown on the horizontal (***X***) and vertical (***Y***) axes. The vector of the magnetic field lies on the axis, perpendicular to the simulation region, and is directed downwards. The degree of shadowing of the figures indicates the module of the velocity in km/s. The results are given for the following moments: (a) $t= 5.2\cdot T_{pe}$, (b) $t= 5.4\cdot T_{pe}$, (c) $t= 5.6\cdot T_{pe}$, (d) $t= 5.8\cdot T_{pe}$.